Diffusion-sensitized magnetic resonance imaging highlights placental microstructural damage in patients with previous SARS-CoV-2 pregnancy infection

Giada Ercolani [a], Silvia Capuani [b,**], Alessandra Maiuro [b,c], Veronica Celli [a], Robert Grimm [d], Daniele Di Mascio [e], Maria Grazia Porpora [e], Carlo Catalano [a], Roberto Brunelli [e], Antonella Giancotti [e], Lucia Manganaro [a,*]

[a] Department of Radiological, Oncological and Pathological Sciences, Umberto I Hospital, Sapienza University of Rome, Italy
[b] CNR ISC Roma Sapienza, Physics Department Rome, Italy
[c] Sapienza University of Rome, Physics Department, Rome, Italy
[d] Siemens Healthcare GmbH, Erlangen, Germany
[e] Department of Maternal and Child Health and Urological Sciences, Sapienza University of Rome, Italy

ABSTRACT

Introduction: Severe acute respiratory syndrome coronavirus-2 (SARS-CoV-2) has been a major global health problem since December 2019. This work aimed to investigate whether pregnant women's mild and moderate SARS-CoV-2 infection was associated with microstructural and vascular changes in the placenta observable in vivo by Intravoxel Incoherent Motion (IVIM) at different gestational ages (GA).
Methods: This was a retrospective, nested case-control of pregnant women during the SARS-CoV-2 pandemic (COVID-19 group, n = 14) compared to pre-pandemic healthy controls (n = 19). MRI IVIM protocol at 1.5T was constituted of diffusion-weighted (DW) images with TR/TE = 3100/76 ms and 10 b-values (0,10,30,50,75,100,200,400,700,1000s/mm2). Differences between IVIM parameters D (diffusion), and f (fractional perfusion) quantified in the two groups were evaluated using the ANOVA test with Bonferroni correction and linear correlation between IVIM metrics and GA, COVID-19 duration, the delay time between a positive SARS-CoV-2 test and MRI examination (delay-time exam+) was studied by Pearson-test.
Results: D was significantly higher in the COVID-19 placentas compared to that of the age-matched healthy group (p < 0.04 in fetal and p < 0.007 in maternal site). No significant difference between f values was found in the two groups suggesting no-specific microstructural damage with no perfusion alteration (potentially quantified by f) in mild/moderate SARS-Cov-2 placentas. A significant negative correlation was found between D and GA in the COVID-19 placentas whereas no significant correlation was found in the control placentas reflecting a possible accelerated senescence process due to COVID-19.
Discussion: We report impaired microstructural placental development during pregnancy and the absence of perfusion-IVIM parameter changes that may indicate no perfusion changing through microvessels and microvilli in the placentas of pregnancies with mild/moderate SARS-Cov-2 after reaching negativity.

1. Introduction

The Coronavirus Disease 2019 (COVID-19) pandemic, due to the Severe Acute Respiratory Syndrome Coronavirus 2 (SARS-CoV-2), has been representing a serious global health concern since December 2019. Despite a large proportion of asymptomatic infections [1], SARS-CoV-2 primarily affects the lungs, inducing a spectrum of respiratory illnesses ranging from mild symptoms to critical respiratory disease and death [2, 3]. Furthermore, accumulating evidence [4] showed that SARS-CoV-2 might also affect other organs expressing the angiotensin-converting enzyme 2 (ACE2) receptor, as SARS-CoV-2 enters cells via the ACE2 receptor. In this scenario, SARS-CoV-2 receptor [5] is also expressed in

maternal-fetal interface cells, such as syncytiotrophoblasts, cyto-trophoblasts, decidual stromal and perivascular cells, endothelial cells, and vascular smooth muscle cells of villi. The co-expression of the viral receptor ACE2 and type II transmembrane serine protease (TMPRSS2) [6] in the human placenta may increase the vulnerability of the placenta to SARS-CoV-2 infection, thus supporting the hypothesis that the placenta is a potential target organ of SARS-CoV-2 infection [7–11].

Moreover, there is increasing evidence that COVID-19 infection leaves signs of maternal vascular malperfusion (MVM), a pattern of placental injury related to abnormal uterine perfusion, leading to pathological changes such as accelerated villous maturation, increased perivillous/intervillous fibrin deposition, decidual vasculopathy, villous infarction, and thrombosis [6,12–24].

The biological plausibility of placental injury in women with SARS-CoV-2 infection has also been confirmed by clinical data showing significantly higher rates of preeclampsia in both asymptomatic and symptomatic women, stillbirths, and perinatal deaths [25,26].

Recently, several studies were focused on the potential of diffusion magnetic resonance imaging (MRI) to study the normal and pathological changes occurring in the placenta and other fetal organs throughout gestation [27–33]. However, to our knowledge, no study has investigated the role of diffusion MRI to assess the placenta of women getting SARS-CoV-2 infection during the COVID-19 pandemic in COVID-19 negative women apart from a work showing a statistically marginal (p = 0.05) altered diffusion coefficient together with a statistically significant difference in blood oxygen level dependent (BOLD) [34].

Diffusion MRI is based on signal attenuation associated with random Brownian motion of water molecules in the presence of magnetic field gradients, to obtain quantitative parameters reflecting the mobility of the water molecules in biological tissues. Among diffusion MRI methods, the IntraVoxel Incoherent Motion imaging (IVIM) [35] allows to separately estimate Brownian diffusion or small-scale diffusion (quantified by the diffusion coefficient, D), large-scale diffusion (quantified by the pseudo-diffusion coefficient, D*) and the regional perfusion effect to the overall diffusion (the perfusion fraction, f) [35]. IVIM MRI considers the signal to be a combination of two signal components: fast-attenuating and slow-attenuating. The fast-attenuating component is associated with small-scale diffusion or blood perfusing in capillaries and is often termed "pseudo-diffusion". The slow-attenuating component is associated with large-scale diffusion of water residing in tissue and is often termed "diffusion" [36]. In highly perfused tissue, such as the placenta, the IVIM model allows the quantification of the diffusion coefficient D not affected by the bias due to perfusion.

Referring to the placental tissue, we can infer that small-scale diffusion occurs in the intra-villous space, and in no-vascular and no-capillaries placental tissue where biological water diffusion is restricted and/or hindered in the extracellular space. On the other hand, large-scale diffusion (or pseudo-diffusion D*) quantifies the perfusion rate of blood flowing through the microcapillary network and inter-villous spaces. Finally, f quantifies the perfusion fraction of water molecules in micro-capillaries and inter-villous spaces while 1-f is related to the diffusion fraction [29,37].

Other methods for assessing placental function are based on $T2$ and T2* relaxometry quantification providing information on the static tissue composition and intrinsic tissue $T2$ and/or T2*value [38,39]. A recent study named Diffusion-rElaxation Combined Imaging for Detailed placental Evaluation (DECIDE) proposed a three-compartment model of placental perfusion that combines $T2$ relaxometry and diffusion imaging [40].

Moreover, machine learning techniques for spectroscopic analysis of quantitative MRI experiments were used to highlight different components in diffusion-relaxometry MRI related to distinct tissue types [41].

This study aimed to evaluate in-vivo the microvascular and microstructure of placental parenchyma in women infected with SARS-CoV-2 during gestation. Towards this goal, patients with previous SARS-CoV-2 pregnancy infection and normal pre-pandemic pregnancies were investigated by IVIM metrics MRI.

2. Materials and methods

2.1. Study design and participants

This was a retrospective, nested case-control of pregnant women with and without SARS-CoV-2 infection during pregnancy enrolled in our Radiology Department between November 2018 and June 2021. We collected all consecutive singleton pregnancies undergoing IVIM MRI after SARS-CoV-2 infection during pregnancy between December 2020 and June 2021 (case COVID-19 group). In the case group, MRI was always performed after a negative swab for SARS-CoV-2. The control group was randomly selected from a cohort of singleton pregnancies undergoing MRI before the SARS-CoV-2 outbreak with MR indications for suspected fetal malformations (ventriculomegaly, corpus callosum abnormalities, renal agenesis, etc.), between November 2018 and October 2019 (control, healthy pre-pandemic group) pregnancies. After the MRI exam, no one of the investigated control group pregnancies showed malformations (ventriculomegaly, corpus callosum abnormalities, renal agenesis, etc.).

The study was approved by the local Ethics Committee of *Sapienza University of Rome* (protocol #0505/2021). All participants were ≥18 years old. Written informed consent from all subjects was obtained in all cases. Gestational age (GA) was assessed by the last menstrual period (LMP). Information about the presence or the absence of fetoplacental Doppler abnormalities at prenatal US assessment was collected. Doppler examination was performed in all pregnancies one week before MRI.

Exclusion criteria were Pregnancy multiple gestations, structural or chromosomal anomalies, suspicion or confirmed fetal vertical infection, or maternal drug intake. We also excluded women with other pregnancy-related diseases (i.e. gestational diabetes mellitus, hypertensive disorders, fetal growth restriction) or pre-existing chronic conditions. Pregnancies with altered placental insertion or adhesive disorders were excluded.

2.2. MRI protocol

Placental MR examinations without maternal-fetal sedation and contrast agents administration were performed on a Siemens MAGNE-TOM Avanto 1.5T scanner (Siemens Healthcare GmbH) using eight coils body probe. Each subject was in a supine position with feet first modality. MRI protocol included T2-HASTE (Half Fourier Single-shot Turbo Spin Echo) without Fat Suppression (FS) and TrueFISP acquisition sequences in para-coronal, para-axial, and sagittal planes on the maternal uterus for the morphological study. T1-weighted images using MPRAGE with and without FS on sagittal and para-axial planes were added to identify the hemorrhagic lacunae's presence.

IVIM protocol included diffusion-weighted (DW) Echo-Planar Imaging (EPI) sequence on the para-axial plane of the maternal uterus including the whole placental surface, with TR/TE = 3100/76 ms; bandwidth = 2174 Hz/px; matrix-size acquisition = 96x96; matrix-size reconstruction = 192x192, number of slices = 30; in-plane resolution = 2.0 × 2.0 mm^2 and slice thickness = 5 mm. The diffusion encoding gradients were applied along 3 directions (x, y, z) using ten different b-values (0, 10, 30, 50, 75, 100, 200, 400, 700, 1000 s/mm^2). The number of averages signal (NS) was NS = 2 for DW images (DWIs) acquired at low b-values (i.e., below b = 200 s/mm^2) and NS = 4 for DWIs acquired at b-value 400, 700, and 1000 s/mm^2. The duration of the IVIM acquisition was about 6 min.

2.3. MRI pre-processing

MR image quality selection and the anatomical identification of maternal and fetal placenta were performed by two radiologists with twenty and six years of experience in prenatal MRI (LM, GE). Since the

reliability of IVIM measurements depends on the signal-to-noise ratio (SNR) of DWI acquired at the maximum b-value, SNRs of DWs acquired at b = 1000 s/mm^2 were evaluated as reported by Capuani et al., 2017 [28]. The mean SNR at b = 1000 s/mm^2 was 11 ± 3 for both healthy and COVID-19 study groups, which is an entirely acceptable value for considering DW data reliable [42] ensuring no-biased IVIM metric values.

2.4. IVIM analysis

DICOM images of DWI acquisitions were elaborated offline with a prototype software named 'Siemens MR Body Diffusion Toolbox' and using a homemade Python script. Fractional perfusion (f), diffusion (D), and pseudo-diffusion (D*) maps were obtained. Signal intensity was averaged in each selected placental ROI (maternal and fetal side placenta), and the function:

$$S(b) / S(0) = f\exp(-b \, D*) + (1 - f)\exp(-b \, D)\text{-}b \, D \qquad (1)$$

was fitted to DWI data. In Eq. (1), S(b) is the diffusion-weighted signal, b is the b-value parameter [27] and S(0) is the signal at b = 0 s/mm^2. The first part of the bi-exponential curve displayed in Eq. (1) describes the perfusion (or large-scale-diffusion) compartment with a rate quantified by D*, and f quantifies the fraction of water molecules pseudo-diffusing in micro-capillaries and small vessels. The second part of Eq. (1) describes the extracellular small-scale diffusion, with a diffusion coefficient D due to (1-f) water molecules. As reported in our previous works [43], we carry out preliminary tests to check the overfitting and stability of the fitting procedure of the experimental data with the function reported in Eq. (1). In particular to obtain maps no preliminary motion correction or Eddy current corrections were performed. The D and f maps were obtained using the procedure explained in Maiuro et al. [43]. Employing a bugged tree algorithm (MATLAB).

Regarding the fitting procedure, a nonlinear least-squares algorithm (Scipy Python's Lib) was used with initial values: S0 = Intensity at b = 0, f = 0, D* = 100, D = 1 and boundary condition: S0 = [0, inf], f = [0,1], D* = [5,10000], D = [0.01,3].

2.5. Statistical analysis

Differences between D, D*, and *f* mean values in the two investigated maternal and fetal placenta ROIs of the healthy and SARS-CoV-2 positive groups were assessed with the Analysis of Variance (ANOVA) test with Bonferroni correction for multiple comparisons. Pearson test with Bonferroni correction was performed to investigate the linear correlation between D, D*, f, and gestational age (GA), body mass index (BMI), COVID duration, and delay time exam+, defined as the delay time between a positive SARS-CoV-2 test and MRI examination.

All statistical analyses were performed using SPSS Statistics 20 (IBM SPSS, Inc. Chicago, IL). Significance was defined as p < 0.05.

3. Results

3.1. Clinical characteristics

The final study cohort was composed of 33 subjects fulfilling the inclusion criteria: 14 SARS-CoV-2 -positive women (COVID-19 group) and 19 healthy pre-pandemic women (healthy control group).

The general characteristics of the two study populations are shown in Table 1 while in Fig. 1 the flow diagram of the subjects investigated. Moreover, Fig. 2 shows an example of maternal and fetal ROI selection in a b = 100s/mm2 (highlighted in yellow) and IVIM D and f maps (highlighted in blue) together with DWI obtained at all the different b-values used to acquire with IVIM protocol.

Apart from the percentage of the C-section, the two study populations had no significant difference in demographic and clinical data.

Table 1

Demographic and clinical data of the investigated women cohort with previous SARS-CoV-2 pregnancy infection (COVID-19 group) and the uninfected healthy pre-pandemic control group.

	Covid-19 (n = 14)	Healthy pre-pandemic (n = 19)	p value
Maternal age (years)	32.5 (22–44)	30 (21–40)	NS
Maternal BMI (kg/m^2)	26 (20–32)	24.05 (20–28)	NS
Blood pressure (systolic/diastolic mmHg)	110/66 (135-80/80-60)	107/68 (120-90/90-50)	NS
GA at MRI (weeks)	30.0 (27.0–36.6)	29.3 (24.4–38.0)	NS
Glycemia (mg/dL)	78.6 (65–93)	74.7 (60–86)	NS
GA at Delivery (weeks)	38.8 (37.6–40)	39 (37.5–41)	NS
C-section (%)	28.6	20	<0.0001
Birth weight (kg)	3.078 (2.640–4000)	3.196 (2.900–4.230)	NS

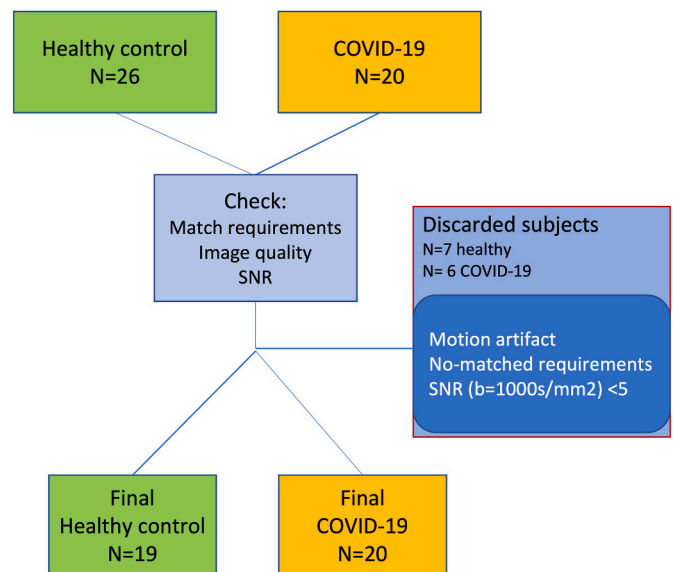Data presented as mean (range).

Fig. 1. Flow diagram of the subjects investigated.

Table 2 shows the main symptoms of each SARS-CoV-2 patient investigated (3/14 were asymptomatic), together with the time interval between positive and negative SARS-CoV-2 test (COVID duration) and the time interval between the positive SARS-CoV-2 swab and MRI exam (delay time exam+).

3.2. Diffusion investigation outcomes

The IVIM parameter D discriminated between the placenta of patients with previous SARS-CoV-2 pregnancy infection and the placenta of healthy subjects, showing significantly higher mean values in the COVID-19 group (see Table 3).

A statistically significant negative correlation was found between D and GA in both the fetal (r = 0.5410, p < 0.036) and maternal (r = 0.6429, p < 0.013) placenta of the COVID-19 group. Conversely, no significant correlation was found between D and GA in normal placentas (Fig. 3). A marginal (p = 0.05) negative correlation was found between D and delay time exam + while a trend of increasing f as a function of delay time exam + was found considering all fetal and maternal placental sites (Fig. 4). Finally, a significant negative correlation (r = 0.92, p < 0.0002) was found between f and COVID duration for SARS-CoV-2 infection duration less than 2.2 months (Fig. 4).
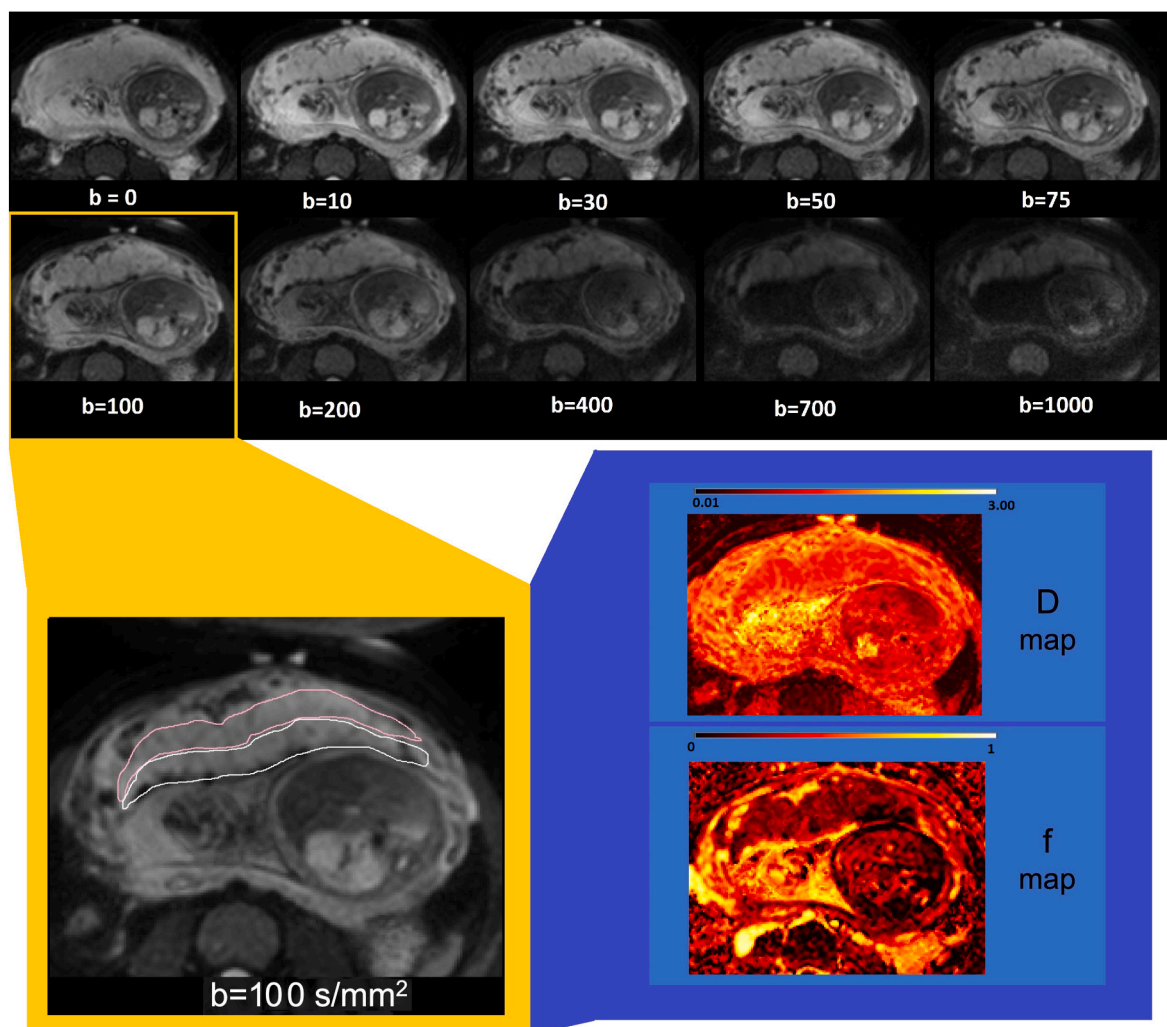
Fig. 2. Top: Example of DWI acquired in a selected subject at different b-values used in the IVIM protocol. Maternal and fetal ROI selection is reported in the b = 100 s/mm^2 image highlighted in yellow. In the blue section of the figure, D (up) and f (below) maps are reported.

Table 2
Specific symptoms experienced by pregnant women during SARS-CoV-2 infection and gestational week (GA) corresponding to the beginning/end of infection, duration of infection, MRI exam, time delay between infection and MRI exam.

	Patient													
	1	2	3	4	5	6	7	8	9	10	11	12	13	14
Symptoms														
fever (>37.5°)		✓	✓		✓	✓			✓		✓			
myalgia						✓							✓	
cold	✓				✓		✓							
cough			✓				✓			✓	✓			
headache			✓						✓					
sore throat													✓	
anosmia ageusia	✓			✓					✓		✓			
dyspnea			✓				✓							
asymptomatic								✓				✓		✓
GA (weeks)														
SARS-CoV-2 RT-PCR +	17.4	17.5	16	21	21.6	3	18.3	19	9.3	24	20.2	21	27.1	20
SARS-CoV-2 RT-PCR −	20	19	19	23	23.3	6	21.3	21	14	26.2	25	23	30.1	23
COVID-19 duration	2.6	1.5	3	2	1.7	3	3	2	4.7	2.2	4.8	2	3	3
MRI exam	27	27	29	29	29	29	29	29	30	30	30	32	34	37
Test + to MRI exam (delay time exam+)	9.6	9.5	13	8	7.4	26	10.7	10	20.7	6	9.8	11	6.9	17

SARS-CoV-2 RT-PCR +, SARS-Cov-2 test positive; SARS-CoV-2 RT-PCR −, SARS-Cov-2 test negative; Test + to MRI exam (delay time exam+), time interval between SARS-Cov-2 test positive and MRI exam.

Table 3

Placental microstructure evaluation by IVIM metrics results in fetal and maternal placenta side of Healthy and COVID-19 group.

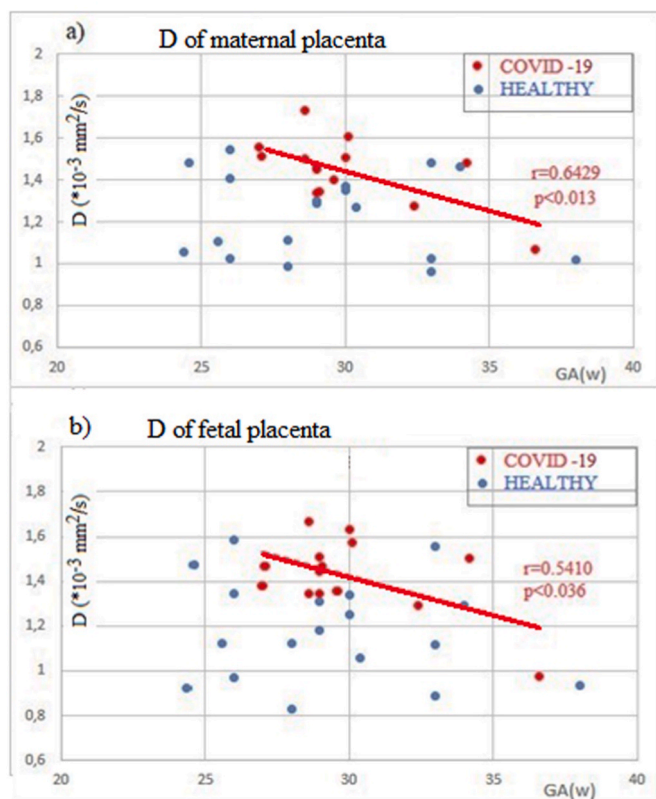|		Healthy[a] (pre-pandemic)	COVID-19[a] positive	*p-value*
Fetal	D ($\bullet 10^{-3}$ mm2/s)	**1.18 ± 0.23**	**1.43 ± 0.17**	**<0.04**
	D[a] ($\bullet 10^{-3}$ mm2/s)	24.98 ± 5.92	26.47 ± 8.95	*NS*
	f (%)	32.70 ± 6.61	31.38 ± 5.82	*NS*
Maternal	D ($\bullet 10^{-3}$ mm2/s)	**1.24 ± 0.20**	**1.45 ± 0.16**	**<0.007**
	D[a] ($\bullet 10^{-3}$ mm2/s)	23.55 ± 5.61	29.50 ± 8.58	*NS*
	f (%)	28.49 ± 5.86	30.53 ± 5.35	*NS*

[a] Data presented as mean ± SD.

Fig. 3. The scatter plots show a significant linear correlation between diffusion coefficient (D) and gestational age (GA) in both maternal (a) and fetal (b) placenta sides of the COVID-19 group. No significant correlation was found between diffusion coefficient (D) and gestational age (GA) in the uninfected control group (Healthy). The solid red line indicates the significant linear correlation with the r and p values displayed.

4. Discussion

4.1. Principal findings

The COVID-19 group of women analyzed in this work had tested positive for SARS-CoV-2 during pregnancy, with consequences ranging from asymptomatic to fever greater than 38° with general exhaustion and hospitalization. None of the patients had been admitted to intensive care. The IVIM MRI protocol was used to investigate the placenta after reaching the negativity of women in the COVID-19 group. In this context, the diffusion coefficient D related to the random movements of the extracellular biological water was statistically higher than that quantified in the placenta of healthy subjects enrolled in the pre-pandemic period (Table 3). Although the increase in D is a nonspecific marker, it is well known that D increases in case of damage to the tissue microstructure. Therefore, in vivo diffusion MRI investigation of previous SARS-CoV-2 positive placentas suggests microstructural placenta damage.

In addition, D showed a negative linear correlation with GA in both maternal and fetal parenchymal sides of the COVID-19 placenta group, depicting a gradual and progressive increment of diffusion restriction with aging, together with no significant correlation between D and GA in the control healthy placentas (Fig. 3). These preliminary results reflect a possible accelerated process of senescence occurring in the COVID-19 compared to the healthy group as already observed in intrauterine growth restriction (IUGR) placentas [29,33].

Although the results do not show an alteration of placental perfusion in COVID-19 group, it seems that f tends to increase with increasing delay time between a positive SARS-CoV-2 test and MRI examination (Fig. 4b), and f increases with decreasing the time interval between positive and negative SARS-CoV-2 test (Fig. 4d). Therefore, timing and duration of infection could affect placental perfusion.

4.2. Results in the context of what is known

The potential of diffusion MRI in vivo is considerable, as demonstrated in numerous contexts ranging from in vivo diagnostics of neurological pathologies involving an alteration of the brain microstructure [44–46] to diagnostics in other human organs and tissues [47, 48]. In agreement with all the vast literature relating to the behavior of the estimated diffusion coefficient D in tissues, the results of the present work suggest that the placentas of women infected by SARS-CoV-2 and negative during pregnancy undergo non-specific damage to the microstructure of the placental parenchyma. According to the current literature [49,50], it may express a mixed-type placental injury characterized by inflammatory-edematous damage associated. In particular, the results reported here agree with the preliminary results of Andescavage et al. [34] that show a trend of increasing D (although not significant) in the COVID-19 group compared to the pre-pandemic control group. IVIM parameters results reported by Andescavage et al. [34] are, in general, higher compared to the results reported here in Table 3. This is most likely attributable to different b values used in the IVIM protocol and to the demographic characteristics of the subjects analyzed. In a recent work by Bouachba et al. [51], several placental lesions due to SARS-Cov-2 infection were analyzed with histopathological examination. The authors conclude that the placentas of COVID-19-positive subjects show diffuse placenta damage, associated with poor fetal outcomes.

4.3. Clinical implications

The quantitative detection of subtle microstructural changes in dysfunctional placentas using the IVIM metric may add useful information about the pathophysiology of pregnancy complications (IUGR, stillbirth …) that could potentially occur in SARS-Cov-2 patients.

4.4. Research implications

Since the subjects analyzed were affected by mild or moderate SARS-Cov-2 symptoms, we did not expect to find differences in IVIM parameters between the pre-pandemic control and COVID-19 groups, or, at most, we expected to find, in agreement with the literature [5,14–17,19, 21–23,26–33], alteration of perfusion parameters. Contrary to expectations, diffusion MRI results underline a clear alteration of D parameter (higher value in SARS-Cov-2 compared to healthy placentas), which can be explained as a microstructural deterioration of the placental tissue. These results, therefore, deserve further investigations that will allow us better to understand the effects of SARS-Cov-2 infection on human
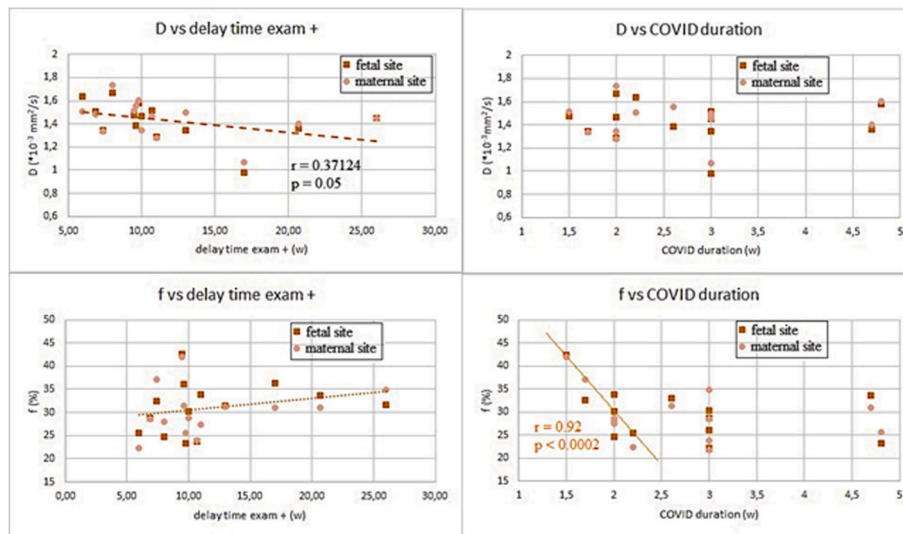
Fig. 4. The scatter plots a) and b) show the behavior of the IVIM parameters D and f as a function of the delay time between a positive SARS-CoV-2 test and MRI examination (delay time exam+) whereas the scatter plots c) and d) show the behavior of D and f as a function of the time interval between positive and negative SARS-CoV-2 test (COVID duration). No significant correlation was found between diffusion coefficient (D) and COVID duration while f showed a significant decrease as a function of COVID duration for a COVID duration less than 2.2 months. Then, f showed a constant value with increasing COVID duration (plot d). The significant correlation is indicated by a solid line with r and p values displayed. The dotted line indicates a linear trend.

tissues.

4.5. Strengths and limitations

The most important limitation of this study is the small group of subjects analyzed. Although the two investigated groups (healthy and COVID-19) are GA-matched, the COVID-19 group is heterogeneous with respect to symptoms caused by COVID-19 infection and viral load. Furthermore, we do not have histopathological examinations of the placentas investigated in vivo.

However, the present study is the first in vivo investigation of COVID-19-affected placentas. It suggests nonspecific microstructural damage with no perfusion alteration in mild or moderate SARS-Cov-2 placentas, in agreement with the subjects' clinical data (i.e., term delivery and normal birth weight).

5. Conclusion

In vivo diffusion MRI in SARS-Cov-2 human placentas highlights nonspecific microstructural damage. According to the current literature [49,50], it may express a mixed-type placental injury characterized by inflammatory-edematous damage. At the same time, the present study suggests an absence of perfusion-related changes across microvessels and microvilli in mild or moderate SARS-Cov-2 placentas when the perfusion is quantified by f IVIM parameter. This behavior agrees with the normality of the clinical data of our study population (i.e., term delivery and birth weight).

In conclusion, the quantification of IVIM parameters showed the potential improvement of our knowledge related to the in vivo microstructural and physiological changes occurring in placentas due to COVID-19 infection.

Declaration of competing interest

The authors declare that they have no known competing financial interests or personal relationships that could have appeared to influence the work reported in this article.

References

[1] Qiuyue Ma, Jue Liu, Liu Qiao, et al., Global percentage of asymptomatic SARS-CoV-2 infections among the tested population and individuals with confirmed COVID-19 diagnosis 4 (12) (December 2021), e2137257.

[2] C. Huang, Y. Wang, X. Li, et al., Clinical features of patients infected with 2019 novel coronavirus in Wuhan, China, Lancet 395 (10223) (2020) 497–506, https://doi.org/10.1016/S0140-6736(20)30183-5.

[3] N. Zhu, D. Zhang, W. Wang, et al., A novel coronavirus from patients with pneumonia in China, 2019, N. Engl. J. Med. 382 (8) (2020) 727–733, https://doi.org/10.1056/NEJMoa2001017.

[4] S. Zaim, J.H. Chong, V. Sankaranarayanan, A. Harky, COVID-19 and multiorgan response, Curr. Probl. Cardiol. 45 (8) (2020), 100618, https://doi.org/10.1016/j.cpcardiol.2020.100618.

[5] M. Hoffmann, H. Kleine-Weber, S. Schroeder, et al., SARS-CoV-2 cell entry depends on ACE2 and TMPRSS2 and is blocked by a clinically proven protease inhibitor, Cell 181 (2) (2020) 271–280, https://doi.org/10.1016/j.cell.2020.02.052. .e8.

[6] E. Taglauer, Y. Benarroch, K. Rop, et al., Consistent localization of SARS-CoV-2 spike glycoprotein and ACE2 over TMPRSS2 predominance in placental villi of 15 COVID-19 positive maternal-fetal dyads, Placenta 100 (2020) 69–74, https://doi.org/10.1016/j.placenta.2020.08.015.

[7] Wastnedge EA, Reynolds RM. Pregnancy and COVID-19. :40..

[8] C. Auriti, D.U. De Rose, C. Tzialla, et al., Vertical transmission of SARS-CoV-2 (COVID-19): are hypotheses more than evidences? Am. J. Perinatol. 37 (S 02) (2020) S31–S38, https://doi.org/10.1055/s-0040-1714346.

[9] N. Ashary, A. Bhide, P. Chakraborty, et al., Single-Cell RNA-seq identifies cell subsets in human placenta that highly expresses factors driving pathogenesis of SARS-CoV-2, Front. Cell Dev. Biol. 8 (2020) 783, https://doi.org/10.3389/fcell.2020.00783.

[10] E. Bloise, J. Zhang, J. Nakpu, et al., Expression of severe acute respiratory syndrome coronavirus 2 cell entry genes, angiotensin-converting enzyme 2 and transmembrane protease serine 2, in the placenta across gestation and at the maternal-fetal interface in pregnancies complicated by preterm birth or preeclampsia, Am. J. Obstet. Gynecol. 224 (3) (2021) 298.e1–298.e8, https://doi.org/10.1016/j.ajog.2020.08.055.

[11] R. Sessa, E. Anastasi, G. Brandolino, et al., What is the hidden biological mechanism underlying the possible SARS-CoV-2 vertical transmission? A mini review, Front. Physiol. 13 (2022), 875806, https://doi.org/10.3389/fphys.2022.875806.

[12] G.N. Algarroba, P. Rekawek, S.A. Vahanian, et al., Visualization of severe acute respiratory syndrome coronavirus 2 invading the human placenta using electron microscopy, Am. J. Obstet. Gynecol. 223 (2) (2020) 275–278, https://doi.org/10.1016/j.ajog.2020.05.023.

[13] F. Facchetti, M. Bugatti, E. Drera, et al., SARS-CoV2 vertical transmission with adverse effects on the newborn revealed through integrated immunohistochemical, electron microscopy and molecular analyses of Placenta, EBioMedicine 59 (2020), 102951, https://doi.org/10.1016/j.ebiom.2020.102951.

[14] A.J. Vivanti, C. Vauloup-Fellous, S. Prevot, et al., Transplacental transmission of SARS-CoV-2 infection, Nat. Commun. 11 (1) (2020) 3572, https://doi.org/10.1038/s41467-020-17436-6.

[15] M. Zaigham, O. Andersson, Maternal and perinatal outcomes with COVID-19: a systematic review of 108 pregnancies, Acta Obstet. Gynecol. Scand. 99 (7) (2020) 823–829, https://doi.org/10.1111/aogs.13867.

[16] P. Zhang, C. Salafia, T. Heyman, C. Salafia, S. Lederman, B. Dygulska, Detection of severe acute respiratory syndrome coronavirus 2 in placentas with pathology and vertical transmission, Am. J. Obstet Gynecol. MFM 2 (4) (2020), 100197, https://doi.org/10.1016/j.ajogmf.2020.100197.

[17] L.M. Ernst, Maternal vascular malperfusion of the placental bed, APMIS 126 (7) (2018) 551–560, https://doi.org/10.1111/apm.12833.

[18] Shanes ED, Mithal LB, Otero S, Azad HA, Miller ES, Goldstein JA. Placental Pathol. COVID-19. :10..

[19] J.J. Mulvey, C.M. Magro, L.X. Ma, G.J. Nuovo, R.N. Baergen, Analysis of complement deposition and viral RNA in placentas of COVID-19 patients, Ann. Diagn. Pathol. 46 (2020), 151530, https://doi.org/10.1016/j.anndiagpath.2020.151530.

[20] R.N. Baergen, D.S. Heller, Placental pathology in covid-19 positive mothers: preliminary findings, Pediatr. Dev. Pathol. 23 (3) (2020) 177–180, https://doi.org/10.1177/1093526620925569.

[21] A. Ferraiolo, F. Barra, C. Kratochwila, et al., Report of positive placental swabs for SARS-CoV-2 in an asymptomatic pregnant woman with COVID-19, Medicina (Mex) 56 (6) (2020) 306, https://doi.org/10.3390/medicina56060306.

[22] J.L. Hecht, B. Quade, V. Deshpande, et al., SARS-CoV-2 can infect the placenta and is not associated with specific placental histopathology: a series of 19 placentas from COVID-19-positive mothers, Mod. Pathol. 33 (11) (2020) 2092–2103, https://doi.org/10.1038/s41379-020-0639-4.

[23] A.L. Hsu, M. Guan, E. Johannesen, et al., Placental SARS-CoV-2 in a pregnant woman with mild COVID-19 disease, J. Med. Virol. 93 (2) (2021) 1038–1044, https://doi.org/10.1002/jmv.26386.

[24] J.E. Mongula, M.W.E. Frenken, G. van Lijnschoten, et al., COVID -19 during pregnancy: non-reassuring fetal heart rate, placental pathology and coagulopathy, Ultrasound Obstet. Gynecol. 56 (5) (2020) 773–776, https://doi.org/10.1002/uog.22189.

[25] A. Conde-Agudelo, R. Romero, SARS-CoV-2 infection during pregnancy and risk of preeclampsia: a systematic review and meta-analysis, Am. J. Obstet. Gynecol. 226 (1) (2022) 68–89, https://doi.org/10.1016/j.ajog.2021.07.009. .e3.

[26] David A. Schwartz, Elyzabeth Avvad-Portari, Pavel Babál, et al., Placental tissue destruction and insufficiency from COVID-19 causes stillbirth and neonatal death from hypoxic-ischemic injury 146 (6) (June 1, 2022) 660–676.

[27] N. Siauve, G.E. Chalouhi, B. Deloison, et al., Functional imaging of the human placenta with magnetic resonance, Am. J. Obstet. Gynecol. 213 (4) (2015) S103–S114, https://doi.org/10.1016/j.ajog.2015.06.045.

[28] S. Capuani, M. Guerreri, A. Antonelli, et al., Diffusion and perfusion quantified by Magnetic Resonance Imaging are markers of human placenta development in normal pregnancy, Placenta 58 (2017) 33–39, https://doi.org/10.1016/j.placenta.2017.08.003.

[29] A. Antonelli, S. Capuani, G. Ercolani, et al., Human placental microperfusion and microstructural assessment by intra-voxel incoherent motion MRI for discriminating intrauterine growth restriction: a pilot study, J. Matern. Fetal Neonatal Med. (March 15, 2022) 1–8, https://doi.org/10.1080/14767058.2022.2050365. Published online.

[30] P.J. Slator, J. Hutter, L. McCabe, et al., Placenta microstructure and microcirculation imaging with diffusion MRI: placenta microstructure and microcirculation imaging, Magn. Reson. Med. 80 (2) (2018) 756–766, https://doi.org/10.1002/mrm.27036.

[31] N. Andescavage, C. Limperopoulos, Emerging Placental Biomarkers of Health and Disease through Advanced Magnetic Resonance Imaging (MRI), 2022, https://doi.org/10.1016/j.expneurol.2021.113868.

[32] G. Ercolani, S. Capuani, A. Antonelli, et al., IntraVoxel Incoherent Motion (IVIM) MRI of fetal lung and kidney: can the perfusion fraction be a marker of normal pulmonary and renal maturation? Eur. J. Radiol. 139 (2021), 109726 https://doi.org/10.1016/j.ejrad.2021.109726.

[33] A. Jakab, R.L. Tuura, R. Kottke, et al., Microvascular perfusion of the placenta, developing fetal liver, and lungs assessed with intravoxel incoherent motion imaging: fetal MRI of Organ Perfusion, J. Magn. Reson. Imag. 48 (1) (2018) 214–225, https://doi.org/10.1002/jmri.25933.

[34] N.N. Andescavage, L. Yuan, S. Barnett, et al., 1116 Microstructural & functional changes in the placenta during the COVID-19 pandemic, Am. J. Obstet. Gynecol. 224 (2) (2021) S687–S688, https://doi.org/10.1016/j.ajog.2020.12.1140.

[35] D. Le Bihan, What can we see with IVIM MRI? Neuroimage 187 (2019) 56–67, https://doi.org/10.1016/j.neuroimage.2017.12.062.

[36] D. Christiaens, P.J. Slator, L. Cordero-Grande, et al., Utero diffusion MRI: challenges, advances, and applications, Top. Magn. Reson. Imag. 28 (5) (2019) 255–264, https://doi.org/10.1097/RMR.0000000000000211.

[37] P.J. Slator, J. Hutter, E. Panagiotaki, M.A. Rutherford, J.V. Hajnal, D.C. Alexander, IVIM MRI of the placenta, in: D. LeBihan, M. Iima, C. Federau, E.E. Sigmund (Eds.), Intravoxel Incoherent Motion (IVIM) MRI, Pan Stanford, New York, 2018, pp. 345–366, https://doi.org/10.1201/9780429427275-16.

[38] I. Derwig, D.J. Lythgoe, G.J. Barker, et al., Association of placental perfusion, as assessed by magnetic resonance imaging and uterine artery Doppler ultrasound, and its relationship to pregnancy outcome, Placenta 34 (2013) 885–891.

[39] M. Sinding, D.A. Peters, J.B. Fr⊘kjær, et al., Prediction of low birth weight: comparison of placental $T2^*$ estimated by MRI and uterine artery pulsatility index, Placenta 49 (2017) 48–54.

[40] A. Melbourne, R. Aughwane, M. Sokolska, et al., Separating fetal and maternal placenta circulations using multiparametric MRI, Magn. Reson. Med. 81 (2018) 350–361, https://doi.org/10.1002/mrm.27406.

[41] P.J. Slator, J. Hutter, R.V. Marinescu, et al., Data-Driven multi-Contrast spectral microstructure imaging with InSpect: INtegrated SPECTral component estimation and mapping, Med. Image Anal. 71 (2021), 102045, https://doi.org/10.1016/j.media.2021.102045.

[42] D.K. Jones, P.J. Basser, "Squashing peanuts and smashing pumpkins": how noise distorts diffusion-weighted MR data, Magn. Reson. Med. 52 (5) (2004) 979–993, https://doi.org/10.1002/mrm.20283.

[43] A. Maiuro, G. Ercolani, F. Di Stadio, A. Antonelli, C. Catalano, L. Manganaro, S. Capuani, Two-compartment perfusion MR IVIM model to investigate normal and pathological placental tissue, J. Magn. Reson. Imag. (2023), https://doi.org/10.1002/jmri.28858.

[44] M. Filippi, Evidence for widespread axonal damage at the earliest clinical stage of multiple sclerosis, Brain 126 (2) (2003) 433–437, https://doi.org/10.1093/brain/awg038.

[45] K.J. van Everdingen, J. van der Grond, L.J. Kappelle, L.M.P. Ramos, W.P.T.M. Mali, Diffusion-weighted magnetic resonance imaging in acute stroke, Stroke 29 (9) (1998) 1783–1790, https://doi.org/10.1161/01.STR.29.9.1783.

[46] M.G. Di Trani, L. Manganaro, A. Antonelli, et al., Apparent diffusion coefficient assessment of brain development in normal fetuses and ventriculomegaly, Front. Physiol. 7 (2019) 160, https://doi.org/10.3389/fphy.2019.00160.

[47] D.M. Koh, D.J. Collins, Diffusion-weighted MRI in the body: applications and challenges in oncology, Am. J. Roentgenol. 188 (6) (2007) 1622–1635, https://doi.org/10.2214/AJR.06.1403.

[48] S. Satta, M. Dolciami, V. Celli, et al., Quantitative diffusion and perfusion MRI in the evaluation of endometrial cancer: validation with histopathological parameters, Br. J. Radiol. 94 (1125) (2021), 20210054, https://doi.org/10.1259/bjr.20210054.

[49] T. Menter, K.D. Mertz, S. Jiang, et al., Placental pathology findings during and after SARS-CoV-2 infection: features of villitis and malperfusion, Pathobiology 88 (1) (2021) 69–77, https://doi.org/10.1159/000511324.

[50] L. Linehan, K. O'Donoghue, S. Dineen, J. White, J.R. Higgins, B. Fitzgerald, SARS-CoV-2 placentitis: an uncommon complication of maternal COVID-19, Placenta 104 (2021) 261–266, https://doi.org/10.1016/j.placenta.2021.01.012.

[51] A. Bouachba, F. Allias, B. Nadaud, et al., Placental lesions and SARS-Cov-2 infection: diffuse placenta damage associated to poor fetal outcome, Placenta 112 (2021) 97–104, https://doi.org/10.1016/j.placenta.2021.07.288.